We are IntechOpen, the world's leading publisher of Open Access books Built by scientists, for scientists

4,800
Open access books available

122,000
International authors and editors

135M
Downloads

Our authors are among the

154
Countries delivered to

TOP 1%
most cited scientists

12.2%
Contributors from top 500 universities

CLARIVATE ANALYTICS BOOK CITATION INDEX INDEXED

WEB OF SCIENCE™

Selection of our books indexed in the Book Citation Index in Web of Science™ Core Collection (BKCI)

Interested in publishing with us?
Contact book.department@intechopen.com

Numbers displayed above are based on latest data collected.
For more information visit www.intechopen.com

11

Modeling of Biological Interfacial Processes Using Thickness–Shear Mode Sensors

Ertan Ergezen et al.*
School of Biomedical Engineering, Health and Sciences, Drexel University, Philadelphia USA

1. Introduction

Biological interfaces and accompanying interfacial processes constitute one of the most dynamic and expanding fields in science and technology such as biomaterials, tissue engineering, and biosensors. For example, in biomaterials, the bio-interfacial processes between biomaterials and surrounding tissue plays a crucial role in the biocompatibility of the layer (Werner, 2008). In tissue engineering, cellular adhesion plays an important role in the regulation of cell behavior, such as the control of growth and differentiation during development and the modulation of cell migration in wound healing, metastasis, and angiogenesis (Hong et al., 2006). Performance of a biosensor is highly dependent on interfacial processes involving the sensor sensing interface and a target analyte. Therefore, quantitative information on the novel and robust immobilization of detector molecules is one the most important aspects of the biosensor field (Kroger et al., 1998).
Thickness shear mode (TSM) sensors have been used in a variety of studies including interfacial biological processes, cells, tissue and properties of various proteins and their reaction (Cote et al., 2003). Phenomena such as cell adhesion (Soonjin et al., 2006.), superhydrophobicity (Sun et al., 2006, Roach et al., 2007), particle-surface interactions (Zhang et al.,2005), organic and inorganic particle manipulation (Desa et al., 2010) and rheological and interfacial properties of blood coagulation (Ergezen et al. 2007) were studied using TSM sensors. Due to the high interfacial sensitivity of TSM sensors, it has been shown that cell motility can be monitored by analyzing the noise of the TSM sensor response (Sapper et al., 2006). It has also been demonstrated that the number of motile sperm in a semen sample can be assessed in real-time using a flow-chamber integrated with a thickness shear mode sensor (Newton et al., 2007).

1.1 Quantification of Thickness Shear Mode (TSM) sensor response

The TSM sensor response is affected by the complex nature of the interface. Its response is influenced by the geometrical and material properties of the interacting surfaces such as surface roughness (Cho et al., 2007), hydrophobicity (Ayad and Torad, 2009), interfacial

* Johann Desa, Matias Hochman, Robert Weisbein Hart, Qiliang Zhang, Sun Kwoun, Piyush Shah and Ryszard Lec
School of Biomedical Engineering, Health and Sciences, Drexel University, Philadelphia USA

slippage (Zhuang et al., 2008), coverage area (Johanssmann et al., 2008), sensitivity profile (Edvardsson et al., 2005) and penetration depth of the shear acoustic wave (Kunze et al., 2006).

Various theoretical models have been developed for quantitative characterization of the TSM sensor response to interfacial interactions. Nunalee et al (2006) developed model to predict of the TSM sensor response to a generalized viscoelastic material spreading at the sensor surface in a liquid medium. Cho et al (2007) created a model system to study the viscoelastic properties of two distinct layers, a layer of soft vesicles and a rigid bilayer. Urbakh and Daikhin (2007) developed a model to characterize the effect of surface morphology of non-uniform surface films on TSM sensor response in contact with liquid. Hovgaard et al (2007) have modeled TSM sensor data using an extension to Kevin-Voigt viscoelastic model for studying glucagon fibrillation at the solid-liquid interface. Kanazawa and Cho (2009) discussed the measurement methodologies and analytical models for characterizing macromolecular assembly dynamics.

The physical description based on a wave propagation concept in a one-dimensional approximation has been proven as the best model of thickness shear mode (TSM) sensors. The fundamentals have been published in several books (Rosenbaum, 1998). Martin et al. have (1994) applied this background to sensors by using Mason's equivalent circuit to describe the thickness shear mode sensor itself and transmission lines as well as lumped elements for viscoelastic coatings, semi-infinite liquids etc.. Follow-up papers have introduced a more straightforward definition of the elements of the BVD-model (Behling et al, 1998) as well as several additional approximations, e.g. based on perturbation theory, to derive less complex equations, have suggested a simplified notation to separate the mass from so-called nongravimetric effects, or have applied the transmission line model to several subsystems (Voinova et al, 2002) for demonstration of specific situations just to call some examples. More recent papers deal with deviations from the one-dimensional approximations, e.g. by introducing generalized parameters by deriving specific solutions e.g. for surface roughness or with discontinuity at boundaries.

TSM sensors combined with the theoretical models mentioned above were used to determine the properties of liquids (Lin et al., 1993), high protein concentration solutions (Saluja et al., 2005), and thin polymer films (Katz et al., 1996).

For viscoelastic layers, their mechanical impedance depends upon the density, thickness, and the complex shear modulus of the loading. Identification of the all the system parameters from the impedance measurements has been very challenging and uncertain without a priori knowledge of the thicknesses and/or some of the material properties (Lucklum et al. 1997).

Furthermore, Kwoun (2006) showed the beneficial features of the multi-resonance operation of the TSM (called as "multi-resonance thickness shear mode) sensor to study the formation of biological samples, specifically collagen and albumin, on the sensor surface. In this work, it was demonstrated that the different harmonic frequency clearly showed the different characteristics of mechanical properties, especially shear modulus, of the biological sample. Although this work was one of the pioneer studies to demonstrate the strengths of the MTSM measurement technique, it is limited as it is a semi-quantitative method. Exact values of mechanical properties of anisotropic collagen and albumin samples were not able to be defined due to complexity of the non-linear simultaneous equations of the model. An improved MTSM technique combined with an advanced data analysis technique was proposed by Ergezen et al (2010). A new approach merging the multi-harmonic thickness

shear mode (MTSM) measurement technique and genetic algorithm-based data analysis technique has been used. This novel method was utilized to solve two unmet needs:

1. Identification of all four parameter by using the MTSM sensor's single harmonic response results in an under-determined problem. The MTSM sensor response enables the identification of two parameters by providing imaginary and real components of the mechanical impedance. In other words, there are fewer equations than the material/geometrical parameters of the interface, therefore, the stochastic method is the only approach that can address this problem mathematically. In this project it was shown that combination of the MTSM measurement technique and the genetic algorithm-based data analysis technique (called as MTSM/GA technique) was used to solve this under-determined problem. *It was reported for the first time, a novel approach that enables determining all four parameters, which define the response of the MTSM technique.*
2. Most of the biological interfaces constitute multi-layer structures. Multi-layer modeling of biological interfacial processes was proposed by several researchers and by us (Wegener et al., 1999, Ergezen et al., 2007). In contrast, there has been very limited (Lucklum et al., 2001) theoretical study and no experimental studies based on the MTSM sensor for quantitative characterization of multi-layer biological processes. *It was reported, for the first time, the most comprehensive theoretical and experimental study for quantitative characterization of multi-layer biological interfacial processes.*

A new approach merging the multi-harmonic thickness shear mode (MTSM) sensor and a data extraction technique based on stochastic global optimization procedure has been proposed. For this purpose, the MTSM/GA technique is being developed and calibrated with a polymer layer (having known properties). This was then used to estimate the properties of a protein layer with unknown properties adsorbed to the MTSM sensor surface. It was demonstrated that this new method has the potential to be a novel tool for quantitatively characterization of interfacial biological layers.

2. Theory

2.1 Multi-Harmonic Thickness Shear Mode (MTSM) sensor

Piezoelectric MTSM sensors transmit acoustic shear waves into a medium under test, and the waves interact with the medium. Shear waves monitor local properties of a medium in the vicinity of the sensor and of the medium/sensor interface (on the order of nm - μm); thus, they provide a very attractive technique to study interfacial processes. Measured parameters of acoustic waves are correlated with medium properties such as interfacial mass/density, viscosity, or elasticity changes taking place during chemical or biological processes.

The shear acoustic wave penetrates the medium over a very short distance. The square of the depth of penetration of an acoustic shear wave in MTSM sensor is related to medium viscosity, elasticity, density and the frequency of the wave (please see Appendix IA.) (Kwoun et al. 2006). Figure 1a shows the acoustic wave penetrating the adjacent medium and Figure 1b shows that the depth of penetration decreases at higher harmonic frequencies in a semi-infinite medium.

Therefore, by changing the frequency, one can control the distance at which the wave probes the medium. Multi-harmonic operation of MTSM sensor will enable to control the interrogating depth into the biological processes. Therefore it will provide a more in depth

characterization of the biological interfacial processes. For example, it was suggested that cell adhesion on extra cellular matrix should be modeled as a multi-layered structure (Wegener et al. 2000). Therefore MTSM sensors can provide information about mechanical and structural properties of the biological processes from different depths (slicing the medium).

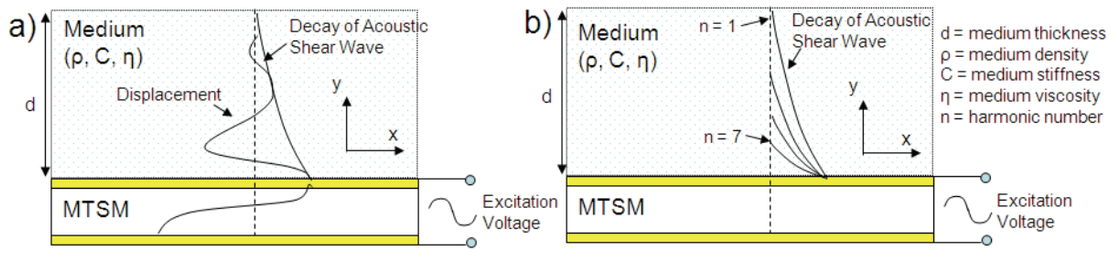

Fig. 1. a) Acoustic wave penetrating into the medium b) depth of penetration decreases at higher harmonic frequencies

It should be noted that it was assumed that the medium is semi-infinite and the mechanical properties are not frequency dependent in fig. 1.

2.2 Electrical response of MTSM sensor

The MTSM sensor is a piezoelectric-based sensor which has the property that an applied alternating voltage (AC) induces mechanical shear strain and vice versa. By exciting the sensor with AC voltage, standing acoustic waves are produced within the sensor, and the sensor behaves as a resonator. The electrical response of the MTSM sensor in air over a wide frequency range is shown in figure 2, where S_{21} is the magnitude response of the MTSM sensor ($|S_{21}|=20\log(100/(100+Z_t))$, Z_t=total electromechanical impedance of the MTSM sensor (Rosenbaum 1998). As an example, the magnitude and phase responses of MTSM sensor are presented at the first (5 MHz), third (15 MHz), fifth (25 MHz) and seventh (35 MHz) harmonics in air.

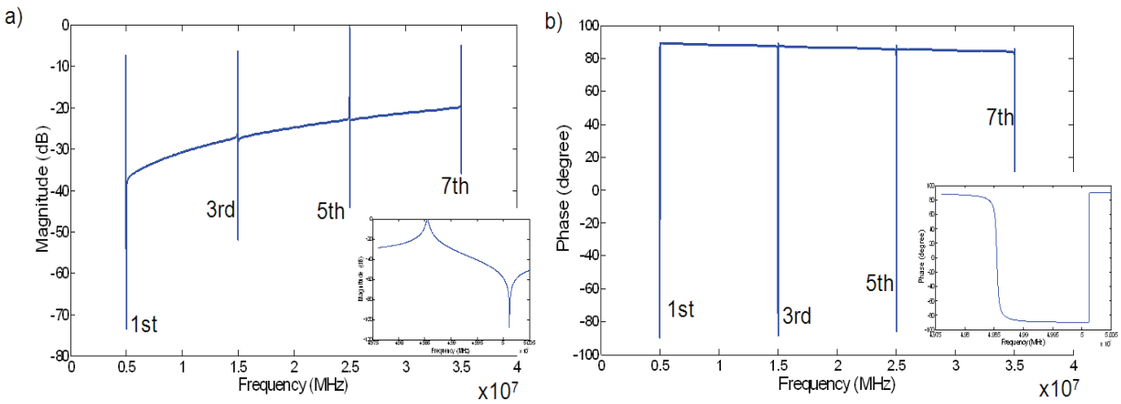

Fig. 2. A typical a) frequency vs. magnitude response and b) frequency vs. phase response characteristic and the associated resonance harmonics for the MTSM sensor, spanning a wide frequency range (5 MHz to 35 MHz). (Insets) Magnified view of magnitude and phase response at 5 MHz

An example of the MTSM's magnitude response in the vicinity of the fundamental resonant frequency is given below (figure 3a). When the TSM sensor is loaded with a biological media, there will be a shift in resonant frequency and a decrease in the magnitude. These changes can be correlated with changes in the mechanical and geometrical properties of the medium such as thickness, viscosity, density and stiffness. Depending on the changes at the interface of the sensor surface-medium interface, a positive and/or negative shift can be seen in the frequency response (Figure 3b).

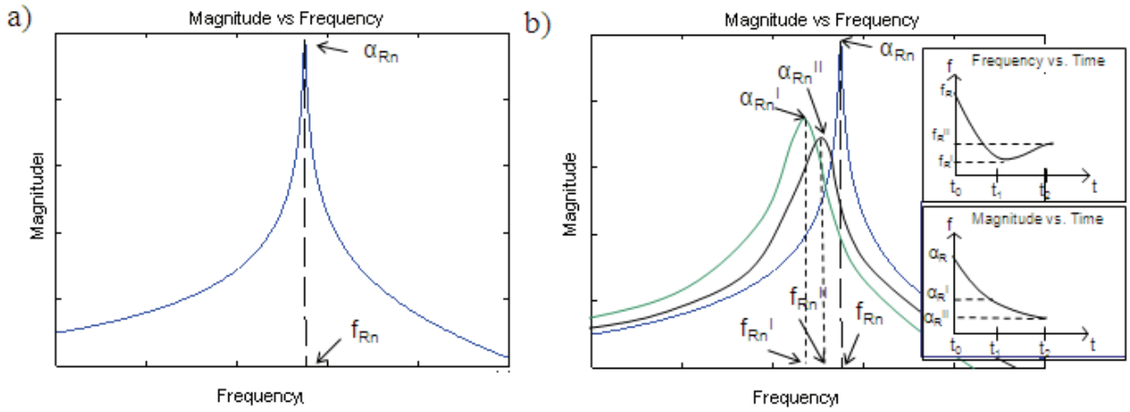

Fig. 3. (a)Demonstration of a typical qualitative frequency-dependent response curve for the MTSM sensor in the vicinity of the resonant frequency; n = harmonic number, α_{Rn}=Initial maximum magnitude, f_{Rn}=Initial resonant frequency, (b) In the case of both positive and negative frequency shifts throughout the experiment, α_{Rn}^{I}, α_{Rn}^{II} =Instantaneous maximum magnitudes of loaded MTSM sensor at time t_1 and t_2 respectively, f_{Rn}^{I}, f_{Rn}^{II} =Instantaneous resonant frequencies of the loaded MTSM sensor at time t_1 and t_2 respectively (Inlet) resonant frequency and magnitude are monitored as a function of time

2.3 MTSM/GA data processing technique

This section will be structured in the following manner; first, the general structure of a genetic algorithm will be explained. Second, advantages of genetic algorithm over other techniques will be discussed. Finally, implementation of MTSM-GA technique for determination of material parameters will be explained.

Principles of operation of a genetic algorithm (GA)

Basic definitions of GA terms are defined in Appendix IB. Genetic algorithm (GA) is based on the genetic processes of biological organisms (figure 4). GA works with a population of individuals, each representing a possible solution to a given problem. Each individual is assigned a fitness score according to how good a solution to the problem it is. The highly-fit individuals are given opportunities to reproduce, by cross breeding with other individuals in the population. This produces new individuals as offspring, which share some features taken from each parent.

Comparison of GA to other data processing techniques

Complex models are ubiquitous in many applications in the fields of engineering and science. Their solution often requires a global search approach. Therefore the objective of optimization techniques is to find the globally best solution of models, in the possible

presence of multiple local optima. Conventional optimization and search techniques include; (1) gradient-based local optimization method, (2) random search, (3) stochastic hill climbing, (4) simulated annealing, (5) symbolic artificial intelligence and (6) genetic algorithms. The detailed information on each technique and comparisons to Genetic Algorithms (GA) are already explained by Depa and Sivanandam (2008). Here, the aim is not to analyze these techniques in detail but to show the suitability of GA as a parameter estimation algorithm. As discussed by Depa and Sivanandam, some of the advantages of GA over other techniques are: (1) it is good for multi-mode problems, (2) it is resistant to becoming trapped in local optima, (3) it performs well in large-scale optimization problems, (4) it handles large, poorly understood search spaces easily. These advantages match with the requirements for an optimization technique to be applied in this application. Therefore GA was chosen as an optimization technique and successfully combined with the MTSM technique.

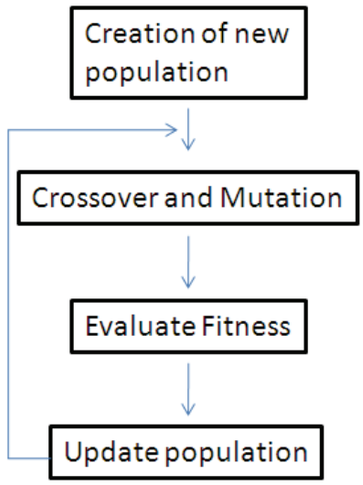

Fig. 4. Flow chart of a genetic algorithm

Structure of the MTSM/GA technique

The structure of MTSM-GA technique is presented in figure 5. As seen from the figure, there are two inputs to the GA, namely; range of variables and MTSM sensor response. GA outputs the determined values of the variables by using GA functions such as crossover, mutation and fitness evaluation. In the following sections, initially, the inputs to the GA will be explained. Then the structure of GA and its internal functions will be presented.

MTSM sensor response

The first input to the GA is the MTSM sensor response. Both magnitude and phase responses were continuously monitored during the experiments (see materials and methods section). Then the specific points on these responses such as resonant frequency, maximum magnitude, minimum phase, frequency at minimum phase, and phase at maximum magnitude were input to GA for calculating the fitness score for each individual. The changes in these target points were calibrated with the diwater/glycerin changes.

Selection of the ranges for variables

The next step of the technique is to set the ranges for the variables (chromosomes). These ranges represent the bounded space within which the GA will search for solutions. The

ranges should be reasonable for each parameter in order to determine accurate solutions. For example, for a Newtonian liquid the stiffness is 0, therefore one should not set the range to be between 1e5 N/m^2 and 1e7 N/m^2. If this were done the algorithm will not converge to a solution because of the inappropriate choice of ranges.

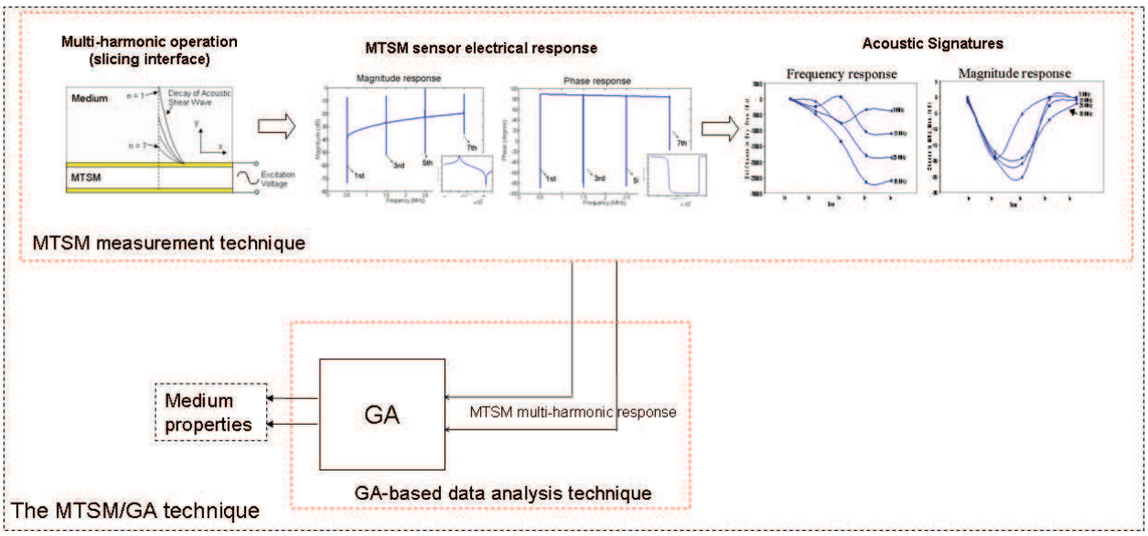

Fig. 5. Basic structure of MTSM/GA technique

As shown by Kwoun (2006), the viscoelastic materials can be divided in to four regimes, namely; liquid like, soft rubber, hard rubber and solid like. As seen from table 1, the viscosity values might change between 0.001 and 0.1 kg/m.s and stiffness value changes between 0 – 1e9 N/m^2 . Typical range of density values for a polymer was determined to be between 1000 – 1400 kg/m^3.

Phase	η (kg/m.s)	C (N/m^2)
Liquid like	0.001 – 0.01	0-1e5
Soft Rubber	0.01 – 0.1	0-1e5
Hard Rubber	0.01 – 0.1	1e5 – 1e7
Solid Like	- 0.1	1e7 – 1e9

Table 1. Four regimes of a viscoelastic system

Genetic Algorithm and its internal functions

This section will be divided into three sections. First, the GA's main parameters such as number of populations, crossovers, mutation rates and genes per chromosome will be analyzed. Then the fitness function of the GA will be explained. Finally, the technique combination of sub-spacing and zooming to determine the values for four variables will be presented.

Selection of GA parameters

Different combinations of the GA parameters were evaluated. Here, the combination that gives the best result is presented. Each variable was represented by a binary chromosome that contains 16 genes. A random population of 100 individuals was generated. Tournament

selection was implemented for selection of individuals for mutation and crossover. In order to carry out the crossovers the entire population is divided into groups of 5 individuals each, these groups are randomly selected. From each group, the individual with the highest fitness together with another individual of this group are selected for crossover. The two selected individuals are the parents and yield two offspring. Both the parents and the offspring pass to the next generation. This idea was implemented in order to reduce the selection pressure.

The crossover between the parents is a simple one meaning that a random crossover point is selected and two kids' genome are formed with the left and right genes of the crossover point of each parent. A relatively high mutation probability (0.5) is present in order to avoid local minimum, otherwise all the individuals might end up having the same genome and this genome corresponding to a not optimal solution. Also elitism was implemented to assure that the best individual of a generation survives to the next generation. This ensures that the algorithm keeps the best solution until a better one is found.

Fitness function

One of the most important parts of a genetic algorithm is the fitness function. The fitness function must reflect the relevant measures to be optimized. This function evaluates the function being searched for the set of parameters of each member of the population. The output of the fitness function is a vector that contains the fitness for each member of the population. This vector helps in the selection of individual for generating new offspring or individuals that will be included in the new generated population.

The approach used, in this study to model biolayers on a MTSM sensor, is Mason's transmission line model (please see Appendix C). This model is a one-dimensional model that describes the electrical characteristics of an acoustic structure wherein, each layer of load can be represented as a T-network of impedances.

Once the initial population is created the algorithm randomly generates a population (includes 100 individuals) chosen from the ranges of the variables (the section titled "selection of the ranges for variables"). Then each individual was input to fitness function (transmission line model). The error between the model (transmission line model) and the experimental results were compared by using the following equation:

$$fit\_func = \frac{100}{1+(\sqrt{(\alpha_{Re}-\alpha_{Rt})^2}+\sqrt{(f_{Re}-f_{Rt})^2}+\sqrt{(P_{Me}-P_{Mt})^2}+\sqrt{(f_{Me}-f_{Mt})^2}+\sqrt{(\alpha_{ARe}-\alpha_{ARt})^2}+\sqrt{(f_{ARe}-f_{ARt})^2})}$$

The denominator of this function represents the difference between the model and the experimental data (we use the plus one in order to avoid the eventual division by zero). In this project, rather than fitting the whole magnitude and phase curve, certain points such as α_R = maximum magnitude, f_R = resonant frequency, P_M = minimum phase, f_M = resonant frequency at minimum phase, α_{AR} = minimum magnitude, f_{AR} = anti-resonant frequency has been compared between the model and the experimental results. Subscript "e" indicates experimental results and subscript "t" stands for theoretical model. This function is monotonously increasing with the kindness of the solution provided by the genetic algorithm. The algorithm was terminated at after 500 generations.

Set-up of the Genetic Algorithm

Acoustic impedance seen at the sensor/film interface is derived from transmission line theory (Martin and Frye 1991). Surface mechanical impedance is related to density and

thickness of the film, and complex modulus (= G^{I} + jG^{II}). Therefore there are four independent variables to define the surface acoustic impedance. The MTSM sensor response contributes two parameters by providing real and imaginary part of mechanical impedance. Hence using single harmonic response results in an under-determined problem. Genetic optimization technique has been applied to under-determined problems to obtain approximate solutions with satisfactory accuracy (Wang and Dhawan, 2008). Here genetic algorithm has been improved by combining sub-space and zooming techniques. It was shown that this combination provides very good approximation with less than 1% error.

First, sub-spacing method was applied. This method gives a quick idea of where the solution can be and also it decreases algorithm running time dramatically (Garaia and Chaudhurib, 2007). Therefore the solution space was divided in 10 sub-spaces. Genetic algorithm was run 5 times in each subspace. Each subspace's convergence performance was evaluated. The sub-space with the best fitness score was considered to be the candidate solution space. It was observed that the candidate sub-space had a distinct convergence performance compared to the others. This method dramatically increased the efficiency of GA by eliminating the irrelevant solution spaces.

Secondly, GA was run 100 times (this number was chosen to have 95% confidence level and 10% confidence interval statistically). The termination criterion for each run was 500 generations. After 100 runs, it was observed that, for two out of four variables, observed points having a uniform distribution (skewness < 0.5) were accumulating around one number in a narrow range (in ±20% of candidate solution point). The average value of the observed points was also equal or very close (<5%) to solution (theoretically shown). Therefore GA was always able to converge to "the most likely" values for two out of four variables after these two steps (from our observations, mostly stiffness and thickness, and sometimes, viscosity and thickness). It was shown theoretically that one can always put these numbers, and calculate the other two variables with the error of less than <15% at this step.

Then zooming method was applied to reduce the search space around the candidate optimum solution point. Several zooming methods have been developed for different applications (Ndiritu and Daniel, 2001, Kwon et al. 2003). In this project, the GA was run 30 times, and then the new range was set to be between maximum and minimum numbers of the 30 points. This zooming continued until the error was less than 1% for all variables. This error was achieved after 6 zooming.

These results showed that the MTMS/GA technique combined with sub-spacing and zooming methods can be applied successfully to approximate the solution with good accuracy for this under-determined problem.

3. Materials and methods

The MTSM/GA technique first experimentally tested with the polymer SU8-2002 layer spin coated on sensor surface. The determined properties of the layer were compared with the values obtained from literature. The technique was then applied to obtain the mechanical and geometrical properties of a protein layer adsorbed on gold layer. The methods and chemicals used in the experiments are described below.

a. Deposition of the thin polymer film

The SU 8-2002 (MicroChem) polymer solution was spin coated on MTSM sensor by using the following procedure. First, the gold electrode surface of TSM sensors was cleaned using

Piranha solution (one part of 30% H2O2 in three parts H2SO4). After 2 min exposure time, the sensors were rinsed with distilled water. The surface was dried in a stream of nitrogen gas. The SU 8 – 2002 sample was dispensed on MTSM sensor surface and sensors were spin coated for 40 seconds. The sensors were then soft baked for 1 min at 95 ^{o}C. The SU 8-2002 films were exposed to UV light for 4 seconds under 25 mJ/cm^2. This was followed by 1 min hard baking on hot plate at 95 ^{o}C.

b. Antibody adsorption on MTSM sensor surface

The reference measurements were taken for air and phosphate buffer saline (PBS). Next, the sensors were exposed to rabit-immunoglobulin G (IgG) (50 µg/ml) suspended in diwater (Fisher Scientific, pH: 5.34, Cat No: 25—555-CM) for 50 minutes to allow IgG coating of the sensor surface by adsorption.

c. Characterization of geometrical properties of the thin film

The thicknesses of the SU 8 – 2002 films were determined by using optical profilometer (Zygo Inc. Model #: NV6200). For the thickness measurements, a very small portion of MTSM sensor surface was not exposed to UV light. After the films were developed, the SU 8-2002 layer was removed from this portion. To obtained different thicknesses of film layer, 1:1 solution of SU8-2002 and cyclopentanone (Acros Organics) was prepared.

The surface topography of the film layer was measured using atomic force microscopy (AFM). The prepared samples were placed on a glass slide installed on the atomic force microscope (Bioscope; Veeco), that was mounted on the inverted fluorescence microscope (TE2000; Nikon, Melville, N.Y.). Measurements were made using contact mode with a scan rate of 2 Hz.

d. Measurement system and MTSM sensor data analysis technique

A 14 mm diameter, 0.33 mm thick, 5 MHz quartz crystal with deposited 7 mm gold electrodes was placed in a custom fabricated brass sensor holder (ICM). The sensor holder was connected to a Network Analyzer (NA) (HP4395A). A LabView program on a personal computer was used to control the network analyzer and collect the data at 5, 15, 25 and 35 MHz. The experiments were done in room temperature (24^{o}C±1^{o}C). Magnitude and phase responses of MTSM sensor were monitored during the experiments (figure 6). The sampling rate was 30 seconds. Each experiment was repeated three times.

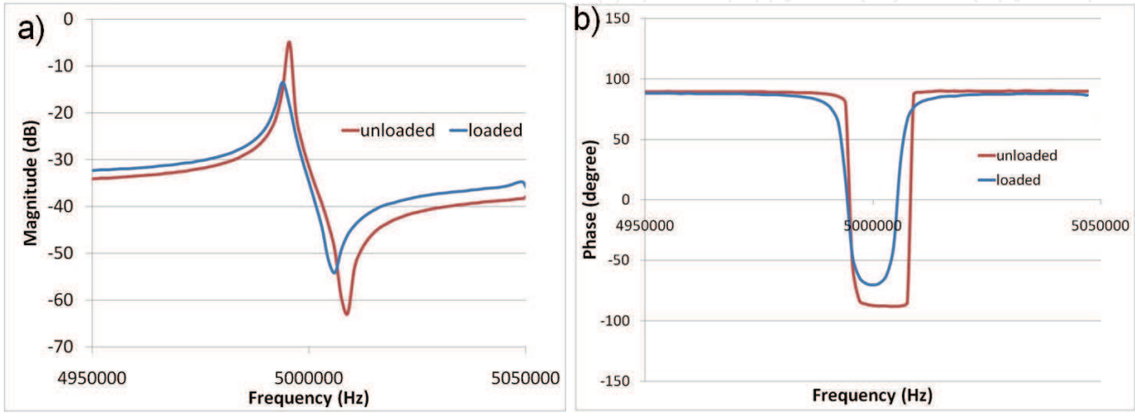

Fig. 6. a) Magnitude and b) phase responses of MTSM sensor

4. Results and discussions

Initially, two different thicknesses of SU8 2002 layers were spin coated on sensor surface and changes in the frequency and magnitude responses were monitored at 5, 15, 25 and 35 MHz. The thicknesses of the layers were measured by using optical profilometer (fig. 7a). The average thicknesses of the layers were 1920±25 nm and 770±50 nm respectively. Surface topography of the SU8 - 2002 layers was measured by using AFM (fig. 7b). The average roughness of the layer was 20 nm and no cracks on the surface were observed.

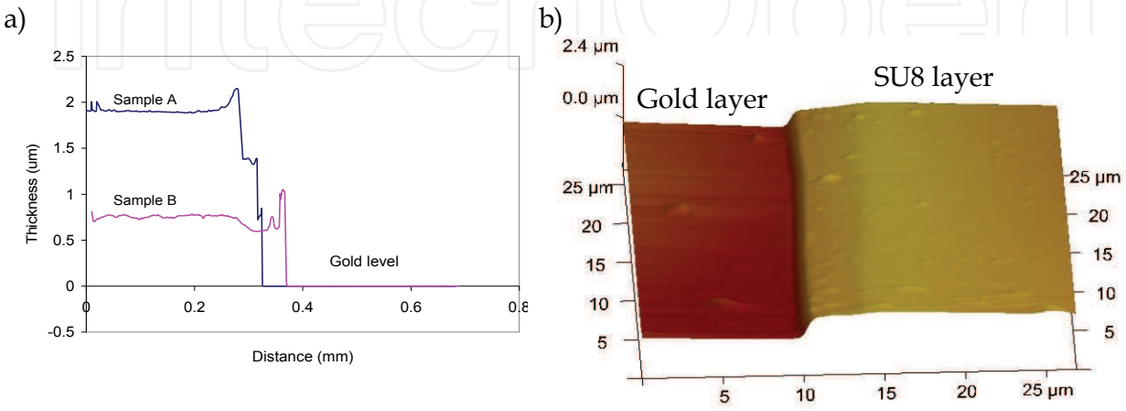

Fig. 7. A) Thickness measurements from optical profilometer sample a. SU8-2000 solution sample b. 1:1 dilution of SU8-2002 and cyclopentanone B) Surface topography of SU 8 layer

a. Determination of mechanical and geometrical properties of SU8 layer of 1.92 µm thickness

First set of experiments were performed by spin coating 2 µm thick SU 8 - 2002 layer on sensor surface. The MTSM/GA determined properties are presented in table 2. The average thickness of the polymer layer determined to range from 2080 nm to 2140 nm among the harmonics. Although these values are slightly higher than the value (1920±25 nm) obtained in control experiments, they are still in less than 10% experimental errors. The variation between the frequencies for density value was also very small, ranging from 1240 to 1253 kg/m^3. These numbers correlate well with the literature value of 1200 kg/m^3 (Jiang et al., 2003) for SU8.

MTSM Frequency	MTSM/GA Results		Profilometer	Jiang et al. [38]
(MHz)	d(nm)	ρ (kg/m^3)	d (nm)	ρ (kg/m^3)
5	2120±60	1253±10	1920±25	1200
15	2140±50	1246±11		
25	2080±110	1240±50		
35	2080±60	1240±28		

Table 2. Comparison density and thickness values of SU 8-2002 layer determined using MTSM/GA sensor at 5, 15, 25 and 35 MHz with profilometer and Jiang et al. (Jiang et al. 2003)

The frequency dependent shear modulus of SU 8-2002 layer obtained using the MTSM/GA is presented in table 3. Both loss and storage modulus varies with the operating frequency. These extracted values were compared with the values obtained by Jiang et al (2003) (table 3). Jiang et al calculated the shear modulus of SU8 layer by using the impedance-admittance characteristics of the equivalent circuit models of loaded and unperturbed TSM sensors operating at 9 MHz.

MTSM Frequency	MTSM/GA Results		Jiang et al.[38] (at 9 MHz)	
(MHz)	G^I (N/m^2)	G^{II} (N/m^2)	G^I (N/m^2)	G^{II} (N/m^2)
5	(4.55±2.12) x10^7	(1.89±0.26) x10^5	7.80e7	2.00e5
15	(2.33±0.18)x10^8	(1.00±0.03) x10^6		
25	(3.82±0.52)x10^8	(4.69±0.52) x10^6		
35	(5.81±0.71) x10^8	(6.49±0.18) x10^6		

Table 3. Comparison of determined G^I and G^{II} values of SU8 layer using MTSM/GA at 5, 15, 25 and 35 MHz and Jiang et al (2003)

As seen in table 3, the values obtained by Jiang et al. fall between the values obtained using the MTSM/GA method for 5 and 15 MHz. The small variation in the G^I and G^{II} may be due to difference in the film preparations. Alig et al. (1996) has shown that variations in film preparation methods can affect the mechanical properties of the polymer layers.

b. Determination of mechanical and geometrical properties of SU8 layer of 0.770 µm thickness

The second set of experiments was done with the ~770 nm thick SU 8-2002 layer on MTSM sensor. As seen from the table 4, the thickness of the layer determined using the MTSM/GA method correlates well with the expected thickness for each harmonic (less than 10% error). Furthermore the results vary only 10 nm between the harmonics. Similarly, determined values for density were consistent between the harmonics, which is around ~1200 kg/m^3.

MTSM Frequency	MTSM/GA Results		Profilometer	Jiang et al.[39]
(MHz)	d(nm)	ρ (kg/m^3)	d (nm)	ρ (kg/m^3)
5	820±45	1180±40	770±50	1200
15	820±20	1190±30		
25	810±35	1190±50		
35	810±52	1213±35		

Table 4. Determined density and thickness values by MTSM/GA or 770 nm thick SU8 layer at 5, 15, 25 and 35 MHz

The initial losses before coating were -0.53 dB and -2.5 dB for 5 and 35 MHz respectively. The losses increase to -0.59 dB for 5 MHz and -4.18 dB for 35 MHz. As seen from these results, the losses remain relatively low when the thickness of the layer was decreased to 770 nm in contrast to the phenomenon observed when the film thickness was 2 µm. For 2 µm

film thickness, the losses increase to -1.9 dB and -11.5 dB at 5 MHz and 35 MHz respectively, while initial loses were similar to what observed for 770 nm film thickness.

The shear modulus values determined via the MTSM/GA technique are presented. Both loss and storage modulus were decreased compared to the values obtained when film thickness was 2 μm (figure 8). It has been shown that the scale effect on the mechanical properties of the polymers might be the reason for the decrease in the values (Liu et al, 2009, Luo et al, 2003).

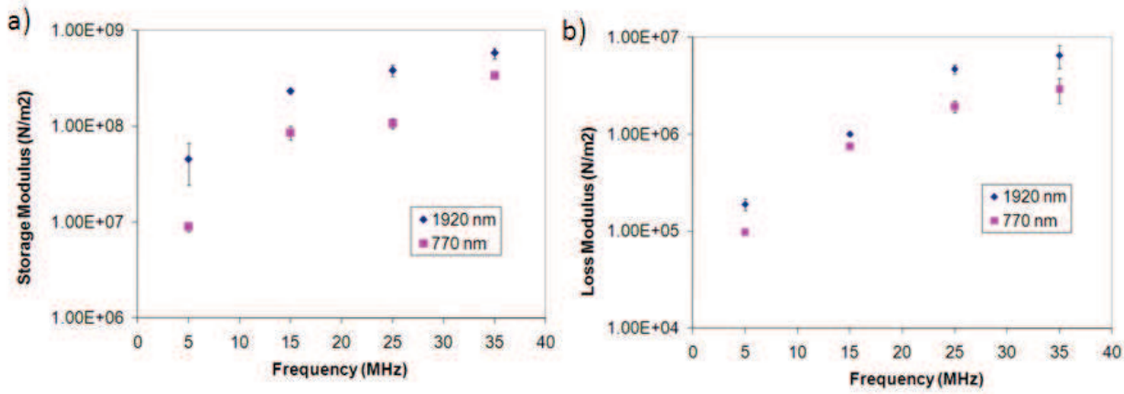

Fig. 8. a) Storage and b) loss modulus as a function of harmonic frequency for 770 nm and 1920 nm thick SU8 layer at 5, 15, 25 and 35 MHz (error bars are smaller than symbols when not visible)

c. Determination of mechanical and geometrical properties of an antibody layer

Third set of experiments were done by adsorbing an antibody layer on MTSM sensor surface under static conditions at 5, 15, 25 and 35 MHz. Antibodies play crucial importance in many applications such as biosensing (Hanbury et al. 1996) and drug delivery (Morrison et al., 1995). The sensor surface was saturated with antibody to form a uniform protein layer on the surface. Change in the frequency and magnitude responses at 15, 25 and 35 MHz are presented in figure 9. At the fundamental frequency (5 MHz), high fluctuations observed in sensor response are likely due to insufficient energy trapping as described by others (Li et al. 2004).

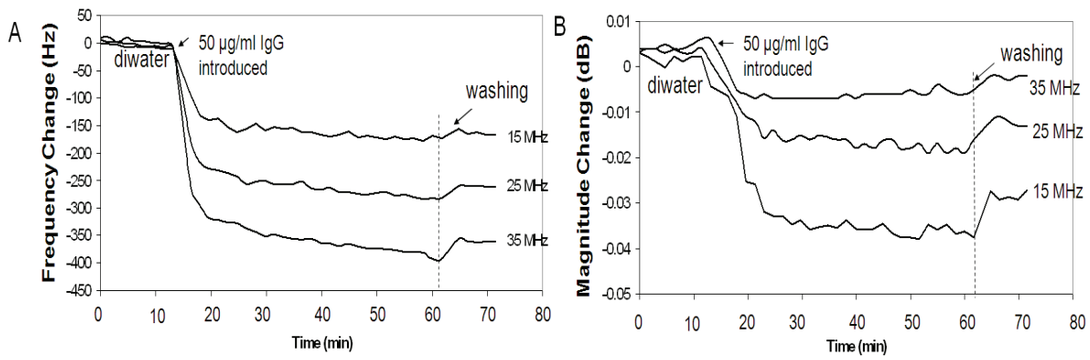

Fig. 9. Time response of A. resonant frequency and B. maximum magnitude responses of MTSM sensor to antibody binding at 15, 25 and 35 MHz

The properties of the medium were determined at t_1 = 10 and t_2 = 70 minutes. At t_1 = 10, the system is modeled as MTSM sensor loaded with semi-infinite Newtonian medium (DIwater) (fig 10A). The height of the column (2 mm) was much higher than the penetration depth of the acoustic wave at 5 MHz (~250 nm in DI water).
At t_2 = 10 min., the MTSM/GA determined properties of the layer at 15, 25 and 35 MHz are presented in table 5. The variations in the determined thickness values were very high (ranging from 300 nm to 5 μm due to the fact that column height was much larger than the penetration depth. Solution range for thickness values was set to be between 1 nm to 10 μm in genetic algorithm. Thus any thickness value larger than the penetration depth will satisfy the solution because the MTSM sensor is not sensitive to the changes beyond the penetration depth. However, the solutions were always higher than penetration depth as expected. Due to the high fluctuations in thickness values, it was not presented here. In contrast the solutions for ρ_1, η_1 and C_1 match with the literature values very well. (Literature values are ρ_1 = 1000 kg/m^3, η_1 = 0.001 kg/m.s and C_1 = 0 N/m^2 at room temperature (Greczylo and Deboswka 2005)).

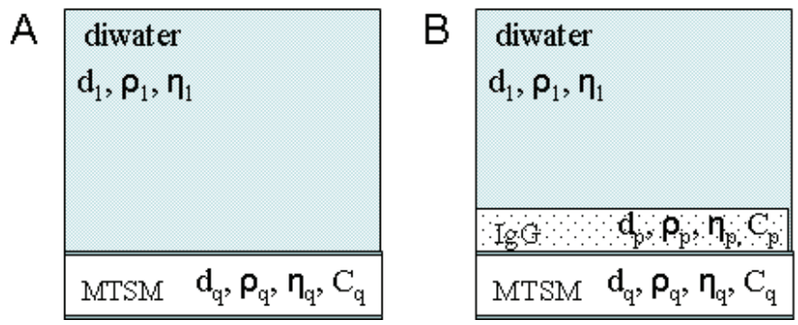

Fig. 10. Physical model for MTSM sensor system at A) t=10 and B) t=70

MTSM Frequency	Density (kg/m^3)	C^l (N/m^2)	η (kg/m.s)
15	1006±5	(2.00±1.00) x10^2	(1.05±.004) x10^{-3}
25	1003±2	(5.00±3.00) x10^2	(1.08±0.03) x10^{-3}
35	1004±4	(1.00±1.00) x10^2	(1.06±0.04) x10^{-3}

Table 5. Determined properties for semi-infinite Newtonian medium layer by MTSM/GA at 15, 25 and 35Hz

At t = 70 min., the physical model is presented in fig 10b. A viscoelastic layer (protein layer) with finite thickness and semi-infinite Newtonian medium were loaded on MTSM sensor. The properties for diwater layer were entered into the algorithm as known variables and the unknown properties (ρ_p, η_p, C_1 and d_p) of viscoelastic layer were determined using the MTSM/GA method. The results are presented in table 6. The thickness of the layer was determined to range from 10.3 to 11 nm for the harmonics. This number correlates well with the values presented by the other researches. Westphal et al (Westphal and Bornmann 2002) calculated the height of antibody layer as 9.2 nm. Furthermore Liao et al (Liao et al 2004) measured the average height of the antibody layer as 10.1±3.3 nm.

The density of the antibody layer was also determined by the MTSM/GA to be 1030±14 kg/m^3. This density value is close to the water density in which the antibodies were suspended. Hook et al. (2002) considered the density of antibody layer as 1050 kg/m^3 when the antibodies were not attached to gold surface. After the cross-linking, the density value was1300 kg/m^3, this is closer to the density value of dry protein. Voros (2004) also showed that the wet density of antibody layer is significantly different than the dry protein density value due to the solvent present in the adsorbed proteins. Therefore we believe that the determined value of the density is in a reasonable range.

MTSM Frequency	Thickness (nm)	Density (kg/m^3)	G^I (N/m^2)	G^{II} (N/m^2)
15	11±0.3	1050±10	(5.20±0.5) x10^4	(4.80±0.58) x10^5
25	10.4±0.6	1080±12	(5.00±0.13) x10^4	(9.50±1.40) x10^5
35	10.3±0.4	1040±14	(5.60±0.12) x10^4	(1.52±0.31) x10^6

Table 6. Determined properties for antibody layer by MTSM/GA at 15, 25 and 35 MHz

As seen from the table 6, the adsorbed antibody layer has low storage modulus (<1e5 N/m^2), and relatively higher loss modulus. While storage modulus was same for each harmonic, loss modulus changed with frequency. It has been experimentally shown that the adsorbed protein layers on TSM sensor, such as antibody, vesicles and cells do not behave like "rigid and thin" films (Voinova et al, 2002). Therefore the linear relationship between resonant frequency shift and mass deposition is not observed. Saluja et al. (2005) indicated low concentrations (less than 60 mg/ml) of antibody suspension behave like Newtonian medium. But it should not be expected that the properties of adsorbed layer will not be the same as the properties of antibody suspension. The effect of the binding between protein layer and gold layer should be considered. No literature value was found for direct comparison. Therefore we believe that MTSM/GA technique will lead to development of a quantitative tool for study of biological interfacial processes.

5. Conclusions

It was shown that MTSM sensor combined with genetic algorithm can be used to extract mechanical and geometrical properties of biological layers. The developed technique was first experimentally tested with SU8-2002 polymer layers with known properties having two different thicknesses. It was shown that the developed technique was successfully determined the mechanical and geometrical layers of thin polymer layers. MTSM/GA technique was then applied to extract the properties of antibody layer coated on MTSM sensor. The obtained data support our hypothesis about use of MTSM/GA technique can be a powerful tool for quantitative characterization of interfacial biological interfacial processes.

6. Acknowledgments

We are thankful to Dr. Moses Noh for providing supplies and micro-fabrication facilities for polymer coating.

7. Appendix I

A. The depth of penetration of a shear wave (δ)

The depth of penetration of a shear wave (δ) in a Newtonian medium is given by the equation shown below:

$$\delta_n = \frac{1}{\left(-\omega_n\left(\frac{\rho_m^2}{C_m^2+(\omega_n\eta_m)^2}\right)^{1/4}\right)Sin\left(-\frac{1}{2}\left(\arctan\left(\omega_n\frac{\eta_m}{C_m}\right)\right)\right)} \quad (2)$$

ρ_m = density of medium (kg/m^3),
η_m = viscosity of medium (kg/m.s),
C_m = stiffness of medium (N/m^2),
ω = angular frequency (rad/s) and
n = harmonic number

B. Basic terminologies of a genetic algorithm

Individual: A solution to the problem is called an individual.
Population: The total number of solutions is called population.
Chromosome: Each individual has a number of chromosomes that represent each parameter (i.e. variables to be determined) of the problem.
Genes: Each chromosome contains a fixed number of genes, the number of genes per chromosome determine the resolution of the total solution. The number of genes per chromosome is mostly determined by the broadness of the range in which each chromosome lies.
Fitness: Every individual has to be weighed according to its fitness. The individual fitness value determines its survival and breeding probability. A higher fitness individual has higher probability of survival.

C. Mason's transmission line model

As seen in fig. 11, the biological process consist of a piezoelectric layer (MTSM sensor) and a non-piezoelectric biological layer. In this model, each layer of load can be represented as a T-network of impedances.

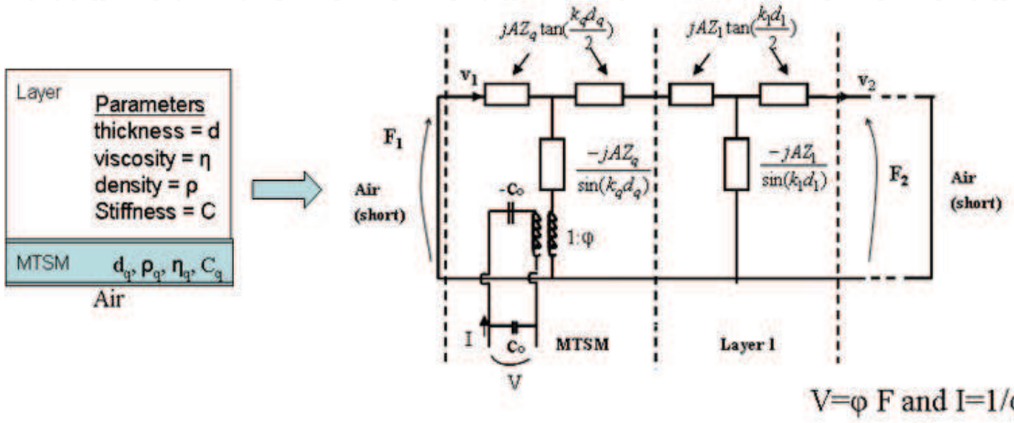

Fig. 11. Mason model representation of non-piezoelectric layers loaded on piezoelectric plate

8. Appendix II (Symbols)

F_1 = input force (N)
F_2 = output force (N)
v_1 = input particle velocity (m/s)
v_2 = output particle velocity (m/s)
A = area of active electrode of MTSM (m^2)
k = propagation constant (m^{-1})
d = thickness (m)
Z = acoustic impedance (acoustic ohm)
I = current (C)
C_0 = static capacitance of MTSM (F)
φ: transformer ratio

9. References

Alig et al, 1996. Ultrasonic shear wave reflection method for measurements of the viscoelastic properties of polymer films. *Rev. Sci. Instrumen*. 68. 1536-1542

Ayad M. M., Nagy L. Torad. 2009. Alcohol vapours sensor based on thin polyaniline salt film and quartz crystal microbalance. *Talanta*. 78. 1280-1285

Behling C, Ralf Lucklum and Peter Hauptmann. 1997. Possibilities and limitations in quantitative determination of polymer shear parameters by TSM resonators. *Sensors and Actuators A: Physical* V. 61, pp. 260-266

Cho N. J., J. Nelson D'Amour, Johan Stalgren, Wolfgang Knoll, Kay Kanazawa, Curtis W. Frank. 2007. Quartz resonator signatures under Newtonian liquid loading for initial instrument check. *Journal of colloid and Interface Science*. 315. 248-254

Cote G. L., R. M. Lec and M. Pishko. 2003. Emerging biomedical sensing technologies and their applications. *IEEE Sensors Journal*. 3. 251-266.

Desa J., Zhang Q., Ergezen E., and Lec. R., 2010 Microparticle manipulation on the surface of a piezoceramic actuator. Measurement Science and Technology. 21 (10) 105803

Dylkov M.S., Sanzharovskii A.T., Zubov P.I. 1966. The effect of thickness on the strength of polymer films. *Mekhanika Polimerov*. 2. 940-942

Edvardsson M., Michael Rodahl, Bengt Kasemo, and Fredrik Ho1o1k. 2005. A Dual-Frequency QCM-D Setup Operating at Elevated Oscillation Amplitudes. *Anal. Chem*. 77. 4918-4926.

Ergezen E, Appel M, Shah P, Kresh JY, Lec RM, Wootton DM, Real-Time Monitoring of Adhesion and Aggregation of Platelets using Thickness Shear Mode (TSM) Sensor, Biosensors and Bioelectronics, V. 23, #4, pp. 575-82, 2007.

Ergezen E. 2010 Multi-Resonant Thickness Shear Mode (MTSM) Measurement Technique for Quantitative Characterization of Biological Interfacial Processes Drexel University, PhD Thesis

Fredriksson, C., S. Kihlman, M. Rodahl, and B. Kasemo. 1998. The piezoelectric quartz Crystal mass and dissipation sensor: a means of studying cell adhesion. *Langmuir*, 14, 248-251.

Galipeau D.W., Vetelino J.V., Lec R. M. and Freger C.1991. The Study of Polyimide Film properties and Adhesion Using a Surface Acoustic Wave Sensors, ANTEC '91,

Conference Proceedings, Society of Plastic Engineers and Plastic Engineering, Montreal, pp. 1679-1984.

Gautam Garaia and B.B. Chaudhurib.2007. Adistributed hierarchical genetic algorithm for efficient optimization and pattern matching. *Pattern Recognition*. 40. 212-228

Greczylo T. and Deboswka E. 2005. Finding Viscosity of liquids from Brownian motion at students' laboratory. *European Journal of Physics*. 26. 827-833

Hanbury C. M., Miller G. W. and Harris B. R. 1996. Antibody characteristics for a continuous response fiber optic immunosensor for theophylline. *Biosensors and Bioelectronics.* 11. 1129-1138.

Hong S., Ertan Ergezen, Ryszard Lec, Kenneth A. Barbee. 2006. Real-time analysis of cell–surface adhesive interactions using thickness shear mode resonator. *Biomaterials*, 27, 5813-5820

Hook F., Larsson C., Fant C., 2002. Biofunctional Surfaces Studied by Quartz Crystal Microbalance with Dissipation Monitoring. *Encyclopedia of Surface and Colloid Science.* 774-790.

Jiang L., Hossenlopp J., Cernosek R., Josse F. 2003. Characterization of Epoxy Resin SU-8 Film Using Thickness-Shear Mode (TSM) Resonator. *Proceedings of IEEE International Frequency Control Symposium.* 996-982

Johannsmann D., Ilya Reviakine, Elena Rojas, and Marta Gallego. 2008. Effect of Sample Heterogeneity on the Interpretation of QCM(-D) Data: Comparison of Combined Quartz Crystal Microbalance/Atomic Force Microscopy Measurements with Finite Element Method Modeling. *Anal. Chem.* 80. 8891-8899.

K. Kanazawa and Nam-Joon Cho. 2009. Quartz Crystal Microbalance as a Sensor to Characterize Macromolecular Assembly Dynamics. *Journal of Sensors.* doi:10.1155/2009/824947

Katz A. and Ward M. D. 1996. Probing solvent dynamics in concentrated polymer films with a high frequency shear mode quartz resonator. *J. Applied Physics*. 80. 4153

D. Kroger, A. Katerkamp, R. Renneberg and K. Cammann. 1998. Surface investigations onthe development of a direct optical immunosensor. *Biosens. Bioelectron.* 13, 1141–1147.

M. Kunze, Kenneth R. Shull, and Diethelm Johannsmann. 2006. Quartz Crystal Microbalance Studies of the Contact between Soft, Viscoelastic Solids. *Langmuir*. 22. 169-173

Kwoun S., 2006. A Multi-Resonant Thickness Shear Mode (MTSM) Sensor for Monitoring The Formation of Biological Thin Films. PhD Thesis, Drexel University, pp. 125.

Li J, Thielemann C, Reuning U, Johannsmann D. 2004. Monitoring of integrin-mediated adhesion of human ovarian cancer cells to model protein surfaces by quartz crystal resonators: evauation in the impedance analysis mode. *Biosens Bioelectron*. 20. 1333–7.

Liao W., Wei F., Qian X. M., Zhao S. X. 2004. Characterization of protein immobilization on alkyl monolayer modified silicaon (111) surface. *Sensors and Actuators B*. 101. 361-367

Lin Z., Yip M. C., Joseph S. I., Ward D. M. 1993. Operation of an ultrasensitive 30 MHz quartz crystal microbalance in liquids. *Anal. Chem*. 65. 1546-1551.

Liu M., Sun J., Bock C., Chen Q. 2009. Thickness dependent mechanical properties of Polydimethylsiloxane. *J. Micromech. Microeng*. 19. 1-4

Lucklum R. and Hauptman P. 1997. Determination of polymer shear modulus with quartz crystal resonators. *Faraday Discussions*. 107. 123-140.

Lucklum R., Peter Hauptmann. 2000. The quartz crystal microbalance: mass sensitivity, viscoelasticity and acoustic amplification. Sensors and Actuators B 70 _2000. 30–36

Luo C., Schneider T., White R., Currie J., Paranjape M. 2003 A simple deflection testing method to determine Poission's ratio for MEMs applications. *J. Micromech. Microeng*. 13. 129-133

Mads Bruun Hovgaard, Mingdong Dong, Daniel Erik Otzen, and Flemming Besenbacher. 2007. Quartz Crystal Microbalance Studies of Multilayer Glucagon Fibrillation at the Solid-Liquid Interface. *Biophysical Journal.* 93. 2162-2169

Martin S.J and G.C. Frye. 1991. Polymer film characterization using quartz resonators. *Ultrasonic. Symp.* 393-398.

Morrison L.S. and Shin S. U. 1995. Genetically engineered antibodies and their applications to drug delivery. *Advance Drug Delivery Reviews.* 15.147-175.

Nam-Joon Cho, Kay K. Kanazawa, Jeffrey S. Glenn, and Curtis W. Frank. 2007. Employing Two Different Quartz Crystal Microbalance Models To Study Changes in Viscoelastic Behavior upon Transformation of Lipid Vesicles to a Bilayer on a Gold Surface. *Anal. Chem.* 79. 7027-7035.

Ndiritu J.G. and Daniell T. M. 2001. An improved genetic algorithm for rainfall-runoff model calibration and function optimization. *Mathematical and Computer Modeling*. 33. 695-706.

Newton M. I., Evans, C.R Simons, Hughes DC. 2007. Semen quality detection using time of flight and acoustic wave sensors. *Applied Physics Letters*. 90 (15) 154103

F. N. Nunalee, Kenneth R. Shull, Bruce P. Lee, Phillip B. Messersmith. 2006. Quartz Crystal Microbalance Studies of Polymer Gels and Solutions in Liquid Environments. *Anal. Chem*. 78. 1158-1166.

Roach, P; McHale, G; Evans, CR, Shirtcliffe NJ, Newton MI. 2007. Decoupling of the liquid response of a superhydrophobic quartz crystal microbalance. *Langmuir*, 23, 9823-9830

Rosenbaum J.F. 1998. Bulk acoustic Wave Theory and Devices. Boston, MA: Artech House Publishers

Saluja A., Kalonia S. D. 2005. Application of Ultrasonic Shear Rheometer to Characterize Rheological Properties of High Protein Concentration Solutions at Microliter Volume. *Journal of Pharmoceutical Sciences*. 94. 1161-1168

Sapper A., Wegener J., Janshoff A., 2006. Cell Motility Probed by Noise Analysis of Thickness Shear Mode Resonators. *Anal. Chem*. 78, 5184-5191.

Sivanandam S. N. and Deepa S. N. 2008. Introduction to Genetic Algorithms. Springer Berlin Heidelberg. New York. 34-35

Song Wang and Atam P. Dhawan. 2008. Shape-based multi-spectral optical image reconstruction through genetic algorithm based optimization. *Computerized Medical Imaging and Graphics*. 32. 429–441

Su H and Thompson M. 1996. Rheological and interfacial properties of nucleic acid films studied by thickness – shear mode sensor and network analysis. *Can. J. Chem*., 74, 344-358

Sun K., R. M. Lec, Cairncross R. A., Shah P., Brinker C. J. 2006. Characterization of Superhydrophobic Materials Using Multiresonance Acoustic Shear Wave Sensors. *IEEE Transactions on Ultrasonics Ferroelectrics and Frequency Control*. 53. 1400- 1403

Szabad, Z. Sangolola, B. and McAvoy, B. 2000. Genetic optimisation of manipulation forces for co-operating robots. *IEEE International Conference on Systems, Man, and Cybernetics*. 5. 3336-3341

Urbakh M. and Leonid Daikhin. 2007. Surface morphology and the quartz crystal microbalance response in liquids. *Colloids and Surfaces A. Physicochemical and Engineering Aspects*. 134. 75-84

Voinova M., Jonson M., Kasemo B., 2002. Missing Mass effect in biosensor's QCM Application. *Biosensors and Bioelectronics*. 17, 835-841

Voros J. 2004. The Density and Refractive Index of Adsorbing Protein Layers. *Biophysical Journal*. 87. 553-561

Yang D., Huang C., Lin Y., Tsaid D., Kao L., Chi C. Lin C., 2003 Tracking of secretory vesicles of PC12 cells by total internal reflection fluorescence microscopy. *Journal of Microscopy*, 209, 223-227

Young-Doo Kwon, Soon-Bum Kwon, Seung-Bo Jin and Jae-Yong Kim. 2003. Convergence enhanced genetic algorithm with successive zooming method for solving continuous optimization problems. *Computers and Structures*. 81. 1715-1725

Wegener, J, et al., 2000. Analysis of the composite response of shear wave resonators to the attachment of mammalian cells. *Biophys. J.* 78, 2821–2833.

Werner C. 2008. Interfacial Phenomena of Biomaterials. *Polymer Surfaces and Interfaces*. Dresden, Germany. Springer-Verlag Berlin Heidelberg. pp. 299

Westphal S. and Bornmann A. 2002. Bimolecular detection by surface plasmon enhanced Ellipsometry. *Sensors and Actuators B*. 84. 278-282

Zhang Q, Desa J., Lec R., Yag G., and Pourrezaei K. 2005, Combination of TSM and AFM for Investigating an Interfacial Interaction of Particles with Surfaces. *Joint IEEE International Frequency control Symposium (FCS) and Precise Tie and Time Interval (PTTI) Systems and Applications Meeting*. 4490454

Zhuang H., Pin Lu, Siak Piang Lim, and Heow Pueh Lee. 2008. Effects of Interface Slip and Viscoelasticity on the Dynamic Response of Droplet Quartz Crystal Microbalances. *Anal. Chem*. 80. 7347-7353

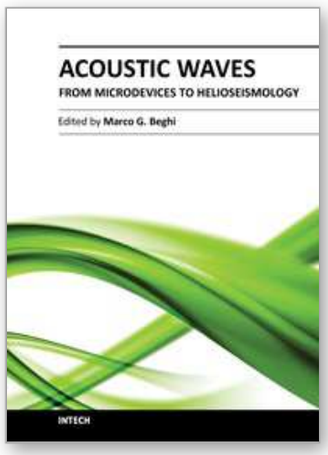

Acoustic Waves - From Microdevices to Helioseismology

Edited by Prof. Marco G. Beghi

ISBN 978-953-307-572-3
Hard cover, 652 pages
Publisher InTech
Published online 14, November, 2011
Published in print edition November, 2011

The concept of acoustic wave is a pervasive one, which emerges in any type of medium, from solids to plasmas, at length and time scales ranging from sub-micrometric layers in microdevices to seismic waves in the Sun's interior. This book presents several aspects of the active research ongoing in this field. Theoretical efforts are leading to a deeper understanding of phenomena, also in complicated environments like the solar surface boundary. Acoustic waves are a flexible probe to investigate the properties of very different systems, from thin inorganic layers to ripening cheese to biological systems. Acoustic waves are also a tool to manipulate matter, from the delicate evaporation of biomolecules to be analysed, to the phase transitions induced by intense shock waves. And a whole class of widespread microdevices, including filters and sensors, is based on the behaviour of acoustic waves propagating in thin layers. The search for better performances is driving to new materials for these devices, and to more refined tools for their analysis.

How to reference

In order to correctly reference this scholarly work, feel free to copy and paste the following:

Ertan Ergezen, Johann Desa, Matias Hochman, Robert Weisbein Hart, Qiliang Zhang, Sun Kwoun, Piyush Shah and Ryszard Lec (2011). Modeling of Biological Interfacial Processes Using Thickness–Shear Mode Sensors, Acoustic Waves - From Microdevices to Helioseismology, Prof. Marco G. Beghi (Ed.), ISBN: 978-953-307-572-3, InTech, Available from: http://www.intechopen.com/books/acoustic-waves-from-microdevices-to-helioseismology/modeling-of-biological-interfacial-processes-using-thickness-shear-mode-sensors

INTECH
open science | open minds

InTech Europe
University Campus STeP Ri
Slavka Krautzeka 83/A
51000 Rijeka, Croatia
Phone: +385 (51) 770 447
Fax: +385 (51) 686 166
www.intechopen.com

InTech China
Unit 405, Office Block, Hotel Equatorial Shanghai
No.65, Yan An Road (West), Shanghai, 200040, China
中国上海市延安西路65号上海国际贵都大饭店办公楼405单元
Phone: +86-21-62489820
Fax: +86-21-62489821

IntechOpen